Kinetic and Dimensional Optimization for a Tendon-driven Gripper

Matei Ciocarlie, Fernando Mier Hicks and Scott Stanford

***Abstract*— We design, optimize and demonstrate the behavior of a tendon-driven robotic gripper performing fingertip and enveloping grasps. The gripper consists of two fingers, each with two links, and is actuated using a single active tendon. During unobstructed closing, the distal links remain parallel, creating exact fingertip grasps. Conversely, if the proximal links are stopped by contact with an object, the distal links start flexing, creating a stable enveloping grasp. We optimize the route of the active tendon and the parameters of the springs providing passive extension forces in order to achieve this behavior. We show how an additional passive tendon can be used as a constraint preventing the gripper from entering undesirable parts of the joint workspace. Finally, we introduce a method for optimizing the dimensions of the links in order to achieve enveloping grasps of a large range of objects, and apply it to a set of common household objects.**

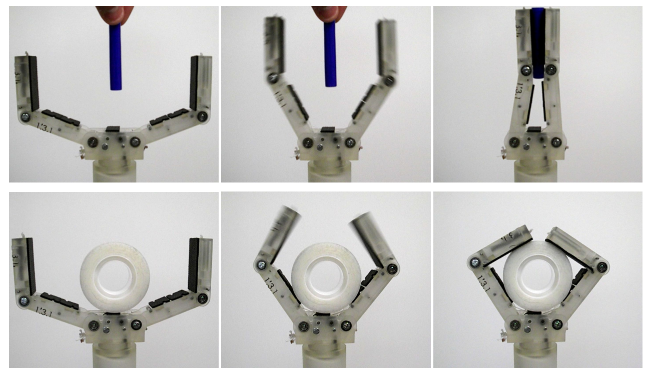

Fig. 1. Fingertip grasp (pen, top row) and enveloping grasp (scotch tape roll, bottom row) performed with the proposed gripper model.

I. INTRODUCTION AND RELATED WORK

End-effectors for robots operating in unstructured environments are typically designed to satisfy multiple criteria. They must be versatile and capable, enabling manipulation of a wide range of objects and in many scenarios. At the same time, low complexity and cost can be key enablers for wide availability, a desirable feature both for research and development, and subsequent refinement into a product.

In this study, we approach end-effector design by starting from the low-complexity end of this spectrum. With the understanding that a gripper populating this part of the design space will inevitably lack a number of advanced capabilities, the features we do add can enable a wide range of tasks and handle many target objects.

We focus on stable grasping, and not in-hand manipulation such as changing the object's pose in hand or activating additional object degrees of freedom (e.g. pushing a button, pulling a trigger). We aim to achieve two types of grasps, which we consider critical for numerous tasks. The first one is fingertip grasps (Fig. 1, top), highly suitable for small objects, or for cases where fingers can not reach around an object (e.g. because of the surface the object is resting on). The second type is that of enveloping grasps (Fig. 1, bottom), creating contacts around the circumference of the object. These grasps are well suited for resisting a wide range of external disturbances, unlike fingertip grasps, which are easily affected by torques applied around the axis of contact.

The hardware starting point consists of two fingers, each with two joints and links. Using at least two revolute joints per finger is motivated by the goal of achieving exact fingertip grasps, where the distal links are perfectly parallel, throughout the range of motion of the fingers. Actuation is performed through a single motor connected to all joints via a tendon, closing (or flexing) the gripper. Opening (or extension) is entirely passive, achieved with joint springs and passive elastic tendons.

With a single motor driving four joints, the hand is underactuated. The choice between the type of grasp being performed (fingertip or enveloping) is not made actively, by controlling the actuators. Rather, it happens passively through object contact, as the hand mechanically adapts to the shape of the object. When the gripper is closing unobstructed, the distal links stay parallel in a fingertip grasp configuration. If the proximal links are stopped by contact with an object, the distal links flex in, completing an enveloping grasp (Fig. 1). Since the ratio of torques applied at each joint can not be changed at run-time, as the joints are not independently actuated, the gripper must be kinetically optimized at design-time for stable grasps in as many cases as possible. We use the term "kinetic" as referring to the effect of net joint torques on both the motion of the fingers and the forces transmitted to an object through contacts.

Passive transition between fingertip and enveloping grasps can also be seen in the highly effective MARS hand [1], which later evolved into the SARAH family of hands [2], both of which use four-bar linkages for actuation. A detailed and encompassing optimization study for underactuated hands, focusing mainly on four-bar linkages but with applications to other transmission mechanisms as well, can be found in [3]. The use of tendons in this study enables a more compact implementation that avoids protruding knuckles, at the cost of reduced finger contact areas.

Perhaps the earliest example of tendon-driven, passively adaptive finger mechanisms is the pioneering work of Hirose and Umetani [4], introducing the Soft Gripper. Passively

All authors are with Willow Garage Inc., Menlo Park, CA. Email: {matei,fhicks,stanford}@willowgarage.com

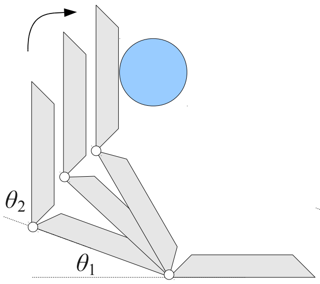

Fig. 2. Desired gripper behaviors: unobstructed closing creating a fingertip grasp (left) and object contact leading to an enveloping grasp (right). As gripper is symmetrical, only one finger is shown.

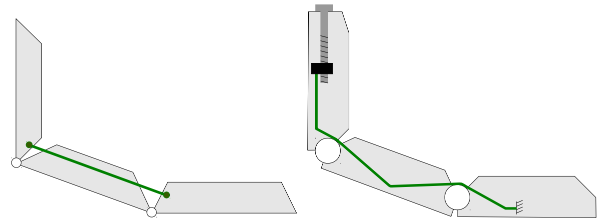

Fig. 3. Hardware implementations of one-sided constraint for fingertip grasping. Left: implementation using a string directly attached to links. Right: implementation via a passive tendon, wrapping around mandrels of equal radii at both joints. One end of the tendon is grounded by a mechanism that allows its length to be adjusted.

adaptive, optimized underactuated designs also include the Harvard Hand [5], [6] and the breakaway transmission mechanism [7] used in the Barrett hand (Barrett Technologies, Cambridge, MA). These designs are highly effective at enveloping grasps, and do not perform fingertip grasps with large and perfectly opposed contact areas.

An important body of work has also focused on the force generation capabilities of redundant or tendon-driven mechanisms in the context of studying the human hand [8], [9], [10], [11]. A number of studies have focused on highly underactuated anthropomorphic hand models [12], [13], [14]; the latter also makes use of the principles of passive adaptation. Finally, force generation has been studied extensively in the context of fully-actuated robotic hands, and a number of useful tools have been proposed; see [15], [16], [17], [18] and references therein for details.

The main contributions of this paper are as follows. We introduce a single-actuator, two-finger gripper capable of both fingertip and enveloping grasps. We present a method for optimizing the route of the active and passive tendons, as well as the stiffness and pretensioning of the extensor springs, for achieving the desired behavior. We use an additional passive tendon as a constraint that prevents the gripper from entering undesirable parts of the joint workspace. We introduce a method for optimizing the absolute and relative dimensions of the links for achieving enveloping grasps of a desired family of objects, and apply it to a large set of common household objects. Finally, we demonstrate a prototype gripper implementing the results of these optimizations.

II. DESIRED OPERATION AND CONSTRAINTS

We use the gripper model shown in Fig. 2; as the fingers are symmetrical, throughout the paper we will focus on the behaviors of a single finger. θ_1 and θ_2 denote the proximal and distal joint angles. A single actuated tendon flexes the joints, with passive springs providing extension torques.

The desired behavior of the gripper can be summarized through four constraints:

1) as the gripper is closing unobstructed, distal links must remain parallel (Fig. 2, left). This means that as the proximal joint flexes, the distal one extends to compensate ($\theta_1 + \theta_2 = 90°$ throughout free motion).
2) if a fingertip grasp has been established, contact forces between the gripper and the object must create a stable grasp. In particular, contact forces on the fingertips should not hyperextend the distal joint ($\theta_1 + \theta_2 = 90°$ must hold in the presence of fingertip contact forces).
3) if proximal joints are stopped due to contact with an object, the distal joint must start flexing (Fig. 2, right) in order to contact the object ($\theta_1 + \theta_2 > 90°$) .
4) once an enveloping grasp has been completed, object contact forces and joint torques created by the tendon must be in equilibrium and create a stable grasp.

We note that, for all constraints above, $\theta_1 + \theta_2 \geq 90°$ is a necessary, but not sufficient condition. This constraint can be enforced with an additional unactuated tendon. The most straightforward implementation is the one shown in Fig. 3 left, with the additional string connecting the palm directly to the distal joint. The mechanism essentially acts as a four-bar linkage, preventing the case where $\theta_1 + \theta_2 < 90°$ throughout the range of motion of the gripper. However, it allows configurations where $\theta_1 + \theta_2 > 90°$, as the string that completes the four-bar simply loses tension and goes slack.

In practice, we implement this constraint with a tendon constrained to wrap around mandrels of equal radii around both joints, as shown in Fig. 3, right. This has the advantage of allowing better control of the tendon route inside the fingers: as long as the tendon wraps around both joint mandrels, the rest of the route can be changed as needed in order to avoid collision with other design elements.

In our optimization and implementation work described below, we attempt to satisfy these constraints in a quasi-static sense. In practice, we have found that at regular operating speeds (*e.g.* gripper closing time of 1s or more) no additional dynamic effects are noticeable. We thus assume that, if the above constraints are met quasi-statically, the behavior of the gripper is fully determined, and can be accurately predicted for a known target object shape and location. In particular, given the starting pose relative to the object, the kinematic behavior dictates which link will first establish contact, and thus the type of grasps that is ultimately obtained.

III. OPTIMIZATION OF KINETIC BEHAVIOR

The hardware constraint described in the previous section contributes significantly to achieving the desired behavior, but does not suffice by itself. In particular, it does not ensure that constraint 1) is met (parallel distal links throughout unobstructed closing), and does not contribute in any way to

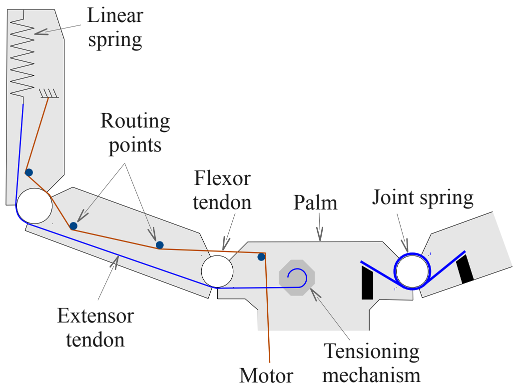

Fig. 4. Gripper components: active tendon (red) with routing points, joint spring (blue) shown at a single joint (on the opposite finger) for clarity, and extensor tendon (blue) connected to linear spring and tensioning mechanism.

constraint 4) (stable contact forces during enveloping grasps). In order to meet all the constraints in the list, and ensure the complete desired behavior, we optimize a number or parameters in the design, pertaining to both the active flexor tendon and the passive, spring-based extension mechanism.

A. *Optimized Design Parameters*

The complete gripper mechanism contains three main components that determine its behavior. The effect of each of these is determined by a number of parameters, detailed in the following list and illustrated in Fig. 4.

1) Flexor tendon. This is the only component connected to a motor, and the only one that can be actively controlled at runtime. We use the common tendon-pulley model (as in [19]), which assumes that the tendon travels through a number of routing points that it can slide through, but that force it to change direction. As a result of this change in direction, the routing points are the locations where the tendon applies force to the links of the finger. The parameters we can optimize are:

- routing point locations. These locations, relative to the joints, determine the joint torques applied by the tendon.
- joint mandrel radii. The tendon can also wrap around joint mandrels. As long as the tendon is touching a mandrel, its moment arm around that joint is constant and equal to the radius of the mandrel. It is possible for the tendon to detach from the mandrel during operation, in which case the moment arm is determined by the routing points proximal and distal to that joint.

2) Joint springs. Each joint contains an off-the-shelf torsional spring, and we can optimize:

- spring stiffness. Changes are made in discrete steps, constrained by availability in manufacturers' catalogs.
- spring pre-tensioning. The springs can be pre-tensioned to exert some level of torque even in the gripper's fully extended pose. We can change the amount of pre-tensioning by varying the location of the spring leg supports inside the links, and by choosing springs with various leg angles at rest.

3) Extensor tendon. In addition to joint springs, extension torques are provided by a passive tendon, running along the extension side of the joint and connected to a linear spring. As this tendon wraps around both joints, it can be used for creating extension forces that depend on the relationship between the joints, unlike torsional springs which affect each joint independently of the other. Also, its moment arms around the joints can be finely controlled through the radii of the joint mandrels. The parameters we optimize are:

- linear spring stiffness. Changes are made in discrete steps, constrained by off-the-shelf availability.
- pre-tensioning level. This is determined by the length of the tendon (and thus the linear spring) in the fully extended pose of the gripper. We have added a pre-tensioning mechanism that allows this parameter to be adjusted after the gripper has been constructed.
- joint mandrel radii. As for the flexor tendon, these determine the constant moment arm of the extensor around each joint. Note that, unlike the flexor tendon, the geometry of the gripper constrains the extensor tendon to always wrap around the mandrels, and additional routing points do not affect its behavior.

We use the parameters in the list above to compute the resulting joint torque $\boldsymbol{\tau}_r = [\tau_1,\ \tau_2]^T$ applied at both joints of the finger, as a function of the joint angles $\boldsymbol{\theta}$ and the actuation force f_a applied to the active tendon. Essentially, the joint torque sums the effect of the active flexor tendon and passive extensor tendon, as well as joint springs:

$$\boldsymbol{\tau}_r\,(f, \boldsymbol{\theta}) = \boldsymbol{J}_a f_a + \boldsymbol{J}_p k_l \Delta l + \boldsymbol{K}_j \Delta\boldsymbol{\theta} \tag{1}$$

where $\boldsymbol{J}_a$ and $\boldsymbol{J}_p$ are the Jacobians of the routing points of the active flexor and passive extensor tendons respectively, k_l and Δl are the stiffness and elongation of the linear spring attached to the extensor tendon, $\boldsymbol{K}_j$ is a diagonal matrix comprising the stiffness coefficients of the joint springs, and $\Delta\boldsymbol{\theta}$ is the vector of joint displacements relative to the rest pose of joint springs.

B. *Joint Torque Ratios and Constraints*

For a given gripper pose and tendon force, the key factor in determining the direction of infinitesimal joint motion or the stability of forces applied to the object is the ratio of individual joint torques τ_1 and τ_2, rather than their absolute values. As such, all of our constraints will be on the normalized value of $\boldsymbol{\tau}_r$ denoted by $\hat{\boldsymbol{\tau}}_r$. We note that $\hat{\boldsymbol{\tau}}_r$ essentially defines a direction in joint torque space; we will express our constraints in terms of this direction.

We check the behavior of the gripper at a number of discrete points throughout its workspace. In particular, we create two sets of poses by taking equidistant samples from the workspace, as illustrated in Fig. 5, left:

- **`fingertip_poses`**: a set of poses where the distal links are parallel, and perpendicular to the palm ($\theta_1 + \theta_2 = 90°$). We note the effect of the hardware constraint that prevents the distal joint from hyperextending (grayed out region in Fig. 5, left).

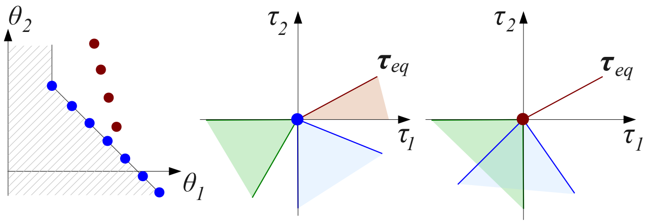

Fig. 5. **Left:** fingertip (blue) and enveloping (red) poses in joint pose space; gripper can not enter grayed out region due to additional tendon constraint from Sec. II. **Middle and right:** joint torque ratio constraints for fingertip (middle) and enveloping (right) poses. We show constraints for parallel closing (blue), grasping (red) and opening (green) regimes.

- **`enveloping_poses`**: a set of poses where the distal joint is flexed for an enveloping grasp; both links make the same angle with the palm axis ($180° - \theta_2 = 2\theta_1$).

In our implementation, the sets contain 11 and 7 poses respectively; we have found this sampling resolution enough to ensure desired behavior throughout the joint workspace.

We also define four levels of active tendon force:

- parallel closing force f_{close}: active force that closes the gripper while maintaining parallel distal links. In this regime, the proximal joint must flex, but the distal joint must extend to compensate.
- enveloping force f_{envel}: active force applied once the proximal links are stopped due to object contact and that flexes the distal joints creating an enveloping grasp.
- grasping force f_{inf}: force applied once an object has been grasped, in order to hold it stably. This can be arbitrarily large, constrained only by the power of the motor and the links' structural rigidity. We consider f_{inf} to be large enough so that the effects of the spring-based forces in the system are negligible. As such, we compute $\boldsymbol{\tau}_r(f_{\text{inf}}, \boldsymbol{\theta}) = \boldsymbol{J}_a f_{\text{inf}}$, ignoring the other terms.
- opening force: for extending the gripper, $f = 0$.

We note that the parallel closing and enveloping regimes imply motion at the joints as a result of the applied tendon force. As such, we assume that part of f_{close} and f_{envel} is used to overcome friction as the tendon slides over the routing points. We assume a constant coefficient of friction between the tendon and all routing points of 0.3.

For every combination of gripper pose and tendon force, we can compute the resultant joint torque $\boldsymbol{\tau}_r(f, \boldsymbol{\theta})$ as in Eq. (1). We also define $\boldsymbol{\tau}_{eq}$, a normalized joint torque resulting from potential contacts with the object:

$$\boldsymbol{\tau}_{eq}(\boldsymbol{\theta}) = \boldsymbol{J}_c \boldsymbol{c} \tag{2}$$

where $\boldsymbol{J}_c$ is the Jacobian of contact locations on the gripper, and $\boldsymbol{c}$ is the vector of contact forces. For fingertip poses, we assume a single contact located in the center of the distal link. For enveloping poses, we assume an additional contact located at the center of the proximal link. We normalize all contact force magnitudes to 1.

We can now compute an overall measure of whether a particular set of design parameters creates the desired behavior. For each pose in the fingertip and enveloping sets, we define the torque ratio constraints explained below, and illustrated in Fig. 6.

For each pose in **`fingertip_poses`** (Fig. 6, middle):

- parallel closing regime: the gripper must stay in the mode where the distal links are parallel, as long as no object is contacted on the proximal links. Thus, the proximal joint must flex, but the distal joint must extend to compensate. This is achieved if f_{close} is strong enough to overcome spring forces at the proximal joint, but not at the distal joint (blue cone).
- enveloping and grasping regimes: tendon force must overcome the spring forces and flex the distal joint as well, once the proximal links have been stopped by contact with the object. However, the ratio of distal to proximal torques must not exceed the level that can be supported by contact with the object (red cone). If τ_2 it too large relative to τ_1, the distal joint will flex and, as in [3], the finger will "eject" from the object. We are not worried about the reverse effect, as the distal joint can not hyperextend due to our hardware constraints.
- opening regime: with no active force applied, the gripper must return to the extended pose (green cone).

For each pose in **`enveloping_poses`** (Fig. 6, right):

- parallel closing regime: the finger must return to a pose where the distal links are parallel (blue cone).
- grasping regime: applied joint torques must be as close as possible to $\boldsymbol{\tau}_{eq}$, the level that can be supported by object contacts (red line). In order to have a stable grasp for frictionless contacts, $\boldsymbol{\tau}_r$ and $\boldsymbol{\tau}_{eq}$ must overlap perfectly. However, in real life, there is always some amount of friction that can be supported at the contact, creating stable grasps even if $\boldsymbol{\tau}_r$ and $\boldsymbol{\tau}_{eq}$ do not overlap perfectly. By trying to bring $\boldsymbol{\tau}_r$ as close as possible to $\boldsymbol{\tau}_{eq}$, we attempt to maximize the set of stable grasps, even for low levels of friction.
- opening regime: the gripper must return to the fully extended pose (green cone).

C. Error Metrics and Optimization Function

To translate the list of constraints above into a function that can be optimized, we must first define error metrics that quantify whether a given constraint is violated. For the constraint that requires $\hat{\boldsymbol{\tau}}_r$ to be as close as possible to $\boldsymbol{\tau}_{eq}$, we minimize the following error metric:

$$\texttt{DIST}(\boldsymbol{\tau}_r, \boldsymbol{\tau}_{eq}, w) = \left(\frac{1 - \hat{\boldsymbol{\tau}}_r \cdot \boldsymbol{\tau}_{eq}}{w}\right)^2$$

where w is a scaling parameter that allows us to determine how quickly the error grows away from the constraint.

The second type of constraint requires $\boldsymbol{\tau}_r$ to be inside a cone, defined for example by $\boldsymbol{\tau}^a$ and $\boldsymbol{\tau}^b$. For satisfying this type of constraint, we attempt to minimize the error metric:

$$\texttt{CNDIST}(\boldsymbol{\tau}_r, \boldsymbol{\tau}^a, \boldsymbol{\tau}^b) = \left(\frac{1 - \hat{\boldsymbol{\tau}}_r \cdot \left(\widehat{\hat{\boldsymbol{\tau}}^a + \hat{\boldsymbol{\tau}}^a}\right)}{1 - \hat{\boldsymbol{\tau}}^a \cdot \left(\widehat{\hat{\boldsymbol{\tau}}^a + \hat{\boldsymbol{\tau}}^b}\right)}\right)^2$$

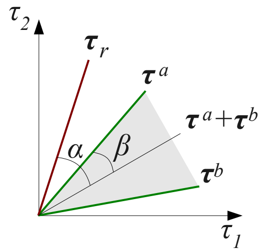

Fig. 6. Angles α and β used to defined a distance metric from the vector $\boldsymbol{\tau}_r$ to the cone defined by $\boldsymbol{\tau}^0$ and $\boldsymbol{\tau}^1$.

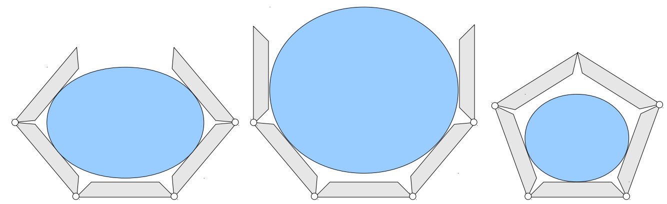

Fig. 7. Examples of enveloping grasps. Left: successful; Middle: object too large, result is equivalent to fingertip grasp; Right: object too small, fingertips collide.

Algorithm 1 Computation of optimization function.

$S = 0$
for all $\boldsymbol{\theta}_i$ in fingertip_poses **do**
  $S \overset{+}{=} \texttt{CNDIST}\left[\boldsymbol{\tau}_r\left(f_{\text{close}}, \boldsymbol{\theta}_i\right),\ (0,-1)^T,\ (1,-0.5)^T\right]^2$
  $S \overset{+}{=} \texttt{CNDIST}\left[\boldsymbol{\tau}_r\left(f_{\text{envel}}, \boldsymbol{\theta}_i\right),\ (1,0)^T,\ \boldsymbol{\tau}_{eq}\left(\boldsymbol{\theta}_i\right)\right]^2$
  $S \overset{+}{=} \texttt{CNDIST}\left[\boldsymbol{\tau}_r\left(f_{\text{inf}}, \boldsymbol{\theta}_i\right),\ (1,0)^T,\ \boldsymbol{\tau}_{eq}\left(\boldsymbol{\theta}_i\right)\right]^2$
  $S \overset{+}{=} \texttt{CNDIST}\left[\boldsymbol{\tau}_r\left(0, \boldsymbol{\theta}_i\right),\ (-1,0)^T,\ (-0.4,-1)^T\right]^2$
end for
for all $\boldsymbol{\theta}_i$ in enveloping_poses **do**
  $S \overset{+}{=} \texttt{CNDIST}\left[\boldsymbol{\tau}_r\left(f_{\text{close}}, \boldsymbol{\theta}_i\right),\ (-1,-1)^T,\ (0.8,-1)^T\right]^2$
  $S \overset{+}{=} \texttt{DIST}\left[\boldsymbol{\tau}_r\left(f_{\text{inf}}, \boldsymbol{\theta}_i\right),\ \boldsymbol{\tau}_{eq}\left(\boldsymbol{\theta}_i\right),\ 1.0e^{-3}\right]^2$
  $S \overset{+}{=} \texttt{CNDIST}\left[\boldsymbol{\tau}_r\left(0, \boldsymbol{\theta}_i\right),\ (-1,0)^T,\ (0,-1)^T\right]^2$
end for
return $\sqrt{S}$

This is equivalent to the formulation

$$\texttt{CNDIST}\left(\boldsymbol{\tau}_r, \boldsymbol{\tau}^a, \boldsymbol{\tau}^b\right) = \left(\frac{1-\cos\alpha}{1-\cos\beta}\right)^2$$

with α and β defined as shown in Fig. 6.

The overall measure is then computed by summing the values of the error metrics for violations of each constraint. The exact formulation, implementing the constraints described in the previous subsection and illustrated in Fig. 5, is shown in Alg. 1. Our optimization goal is to find the set of parameters that minimize the resulting value of S.

D. Optimization Method

We perform the optimization using a combination of random search and gradient descent with numerical gradient computation. At each step, a random set of parameters is chosen and the corresponding value of S is computed. If S is below a given threshold, we run a gradient descent loop, where a step is taken in the direction of the numerically computed gradient until S stops improving. The resulting parameter set is then saved into a database. The overall algorithm can be allowed to run for an arbitrarily chosen amount of time, after which point the configuration with the lowest value of S found so far can be used.

In practice, for a parameter space of dimensionality 16, we have found that one computation of the function S takes approximately 19ms, while computation of the numerical gradient takes approximately 0.6s. We have not performed a rigorous analysis of the time required for the best solution to stop improving; empirically, we have found that after approximately 60 CPU hours of computation (8 to 10 hours on a single multi-core commodity desktop) no significant improvements can be obtained.

In future work, we plan to try different optimization algorithms suited for large dimensional parameter spaces and highly non-linear optimized functions, such as simulated annealing. Other possible approaches could include casting the optimization function to a formulation that allows efficient computation of the global optimum, such as a Linear or Quadratic Program, as in [20].

IV. OPTIMIZATION OF LINK DIMENSIONS

Based on the kinetic optimization described so far, the gripper we are proposing can execute both fingertip and enveloping grasps. The main reason for pursuing these capabilities is to increase the versatility of the gripper; however, in order to maximize their benefit we must also focus on the range of objects that such grasps can be executed on.

Fingertip grasps are relatively straightforward in terms of graspable object dimensions: the widest object that can grasped must fit between the fingers in the fully extended pose; the thinnest one can be arbitrarily thin (e.g. a sheet of paper). However, enveloping grasps are more difficult to execute. Fig. 7 illustrates potential successful and unsuccessful enveloping grasps based on the dimensions of the grasped object. The determining factors for the range of objects that the gripper can geometrically envelop are the lengths and thicknesses of the links. We propose a second type of optimization, aiming to maximize this range.

We parameterize the space of possible objects by dividing their 2D profiles into two categories: rectangular and elliptical. For each category, the object profile is defined by its width and height.

The parts of the object space that are most important for a gripper to cover will be application-specific. For a gripper intended for versatile manipulation in human settings, we measured a set ($n = 62$) of objects common in households and offices, such as glasses, mugs, bottles, pens, cellphones, various product boxes, staples, computer mice, etc. An illustration of the 2D rectangular and elliptic object spaces is shown in Fig. 8, populated by the objects we measured.

A. Optimization Function

We optimized 6 parameters that affect the space of objects the gripper can geometrically enclose: length and thickness

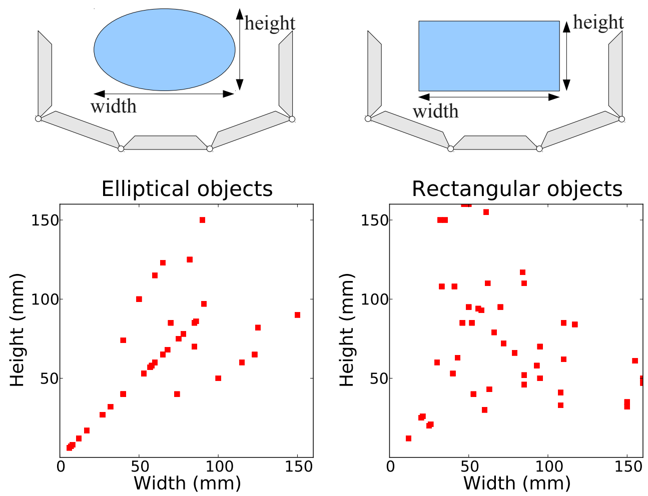

Fig. 8. Space of rectangular and elliptical object profiles, populated by common household objects such as cans, bottles, pens, condiment packs, etc. Spaces are symmetrical, as objects can be approached from either direction.

of the palm, proximal and distal links. For each set of parameters, the optimization function was defined as the number of discrete samples in the object space interest region that the gripper failed to enclose. Each object was approached by the gripper along a direction aligned with its height axis, and centered along the object's width. An enveloping grasp was defined as successful if:

- contact is established on all four links of the gripper.
- $\theta_1 \geq 45°$: as the gripper is underactuated, the proximal joints stop flexing only when contact with an object prevents further motion; only at that point do the distal joint start flexing. The exact angle where that happens depends on the friction coefficient between the proximal link and the object. We chose a value of $45°$, which corresponds to a friction coefficient of 1.
- $\theta_1 + \theta_2 \geq 110°$: this condition distinguishes an enveloping grasp from a fingertip grasp (Fig. 7, middle).
- the opposing fingertips do not collide as they are flexing to complete the enveloping grasp (Fig. 7, right).

Based on the distribution of measured objects, we empirically defined the following object space regions of interest:

- we noted that circular objects are more predominant than non-circular elliptical ones. We thus focused on circular objects with diameters between $40mm$ and $90mm$, sampled every $10mm$. Objects with diameters between $50mm$ and $60mm$ were given double weight (69 discrete samples in total).
- rectangular objects with width and height between $40mm$ and $100mm$, independently sampled at every $10mm$ (49 samples in total).

It is important to note that this type of object space sampling is far from complete. It does not explicitly address objects with irregular shapes, or objects approached by the gripper along a direction that is offset from the center and not aligned with a major object axis. In practice, we have found that explicitly optimizing for this particular subset of object

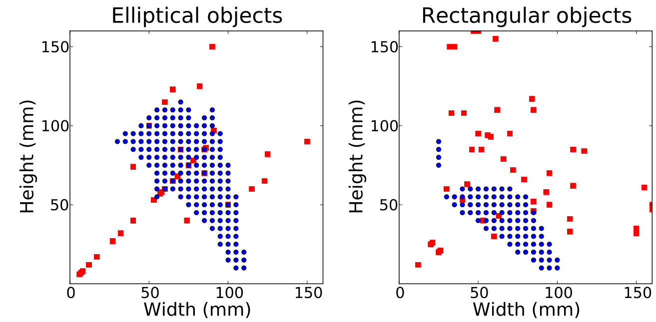

Optimized gripper with dimensions from Table I

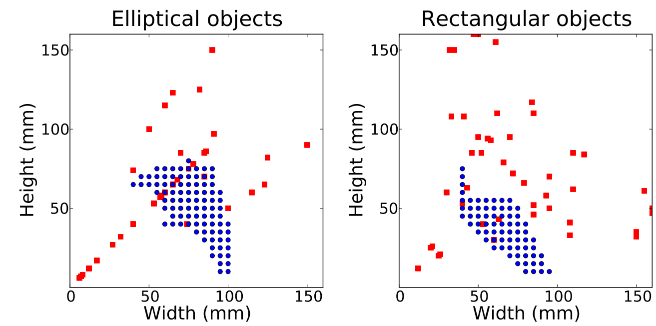

Unoptimized gripper, all links 50mm long and 8mm thick.

Fig. 9. Space of objects that a gripper can enclose in an enveloping grasp (blue), superimposed on samples of objects common in households and offices (red).

	Palm	Prox. link	Dist. link
Length (mm)	35	65	53
Thickness (mm)	9	8	7

TABLE I
DIMENSIONS FOR OPTIMIZED GRIPPER.

shapes, and relying on the gripper's passive mechanical adaptation to handle deviations from it, works well in a wide range of situations, as we will illustrate in the next section.

We also note that the space of enveloping grasps is always complemented by the space of fingertip grasps, which is significantly less constrained. This is the reason why we chose to focus enveloping grasps on the relatively large objects in our set, with an assumption that fingertip grasps are well suited for small objects.

B. Optimization Results

We used the same optimization method described in Sec. III-D, with the parameters and function described in the previous subsection. For this function, a single evaluation took approximately 0.25s, and computation of the numerical gradient took approximately 3s. We allowed complete optimization times similar to the ones in Sec. III-D.

The best parameter values we found are shown in Table I. The corresponding ranges of objects that the gripper can envelop are shown in Fig. 9. For comparison, we also show the same plot for an unoptimized gripper, with all link lengths equal to 50mm and thicknesses equal to 8mm.

We notice that the optimization method produces improved coverage of the object space, allowing for enveloping grasps

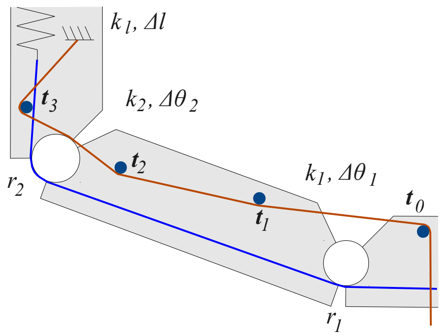

Fig. 10. Notations used for parameters of prototype gripper.

param.	t_{0x}	t_{0y}	t_{1x}	t_{1y}	t_{2x}	t_{2y}	t_{3x}	t_{3y}
value	-25.0	6.0	-45.0	3.6	-7.6	0.9	-42.0	-5.0

param.	k_1	$\Delta\theta_1$	k_2	$\Delta\theta_2$	k_l	$\Delta\theta_l$	r_1	r_2
value	9.9	4.5	4.5	4.3	0.24	12.0	2.4	3.2

TABLE II

PARAMETER VALUES FOR OPTIMIZED GRIPPER.

of a wide range of objects. However, many common objects still can not be enveloped; for those, this particular model must rely on fingertip grasps. In the future, we plan to study additional methods for improving the range of objects we can envelop; these can include overlapping fingers, interlocking distal links, or multiple fingers offset from each other in the plane perpendicular to the closing direction, as in [6].

V. PROTOTYPE AND DEMONSTRATION

In order to build a gripper with the desired characteristics, we first ran the optimization presented in the previous section resulting in the set of desired link dimensions. Then, based on these results, we ran the kinetic optimization presented in Sec. III, computing the parameters of the actuation mechanism. Using the notation in Fig. 10, the parameters used for the kinetic optimization were:

- $\boldsymbol{t}_{0..3}$: location of tendon routing points relative to link coordinate systems (mm). The palm coordinate system (used for t_0) is located at the proximal joint; the proximal link's coordinate system (used for t_1 and t_2) is located at the distal joint, and the distal link's coordinate system (used for t_3) is located at the fingertip. In each case, x is parallel with the bottom of the corresponding link and pointing away from the palm, and z is the joint's axis of rotation, with positive rotation around z corresponding to flexion.
- $k_{1,2}$, $\Delta\theta_{1,2}$: stiffness (Nmm/rad) and pre-tensioning (rad) of joint torsional springs.
- k_l and Δl: stiffness (N/mm) and pre-tensioning (mm) of linear spring attached to extensor tendon.
- r_1, r_2: radii (mm) of proximal and distal joint mandrels.

The best configuration found is presented in Table II.

The value of the dimensionless optimization function S, computed using Alg. 1 for this configuration is 3.47. This value represented the norm of the error metrics computed over a set of 18 poses (11 fingertip grasps and 7 enveloping grasps), according to multiple constraints for each pose. As such, it is difficult to attach intuitive insights to any particular value. We do note however that each individual error metric was defined so that a value below 1.0 indicates qualitatively acceptable behavior; as such, we take a norm of 3.47 over 64 total constraints to be acceptable, a result that was indeed confirmed in practice, as we show below.

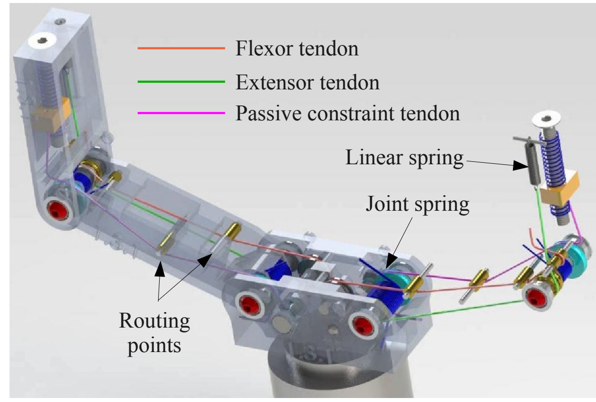

Fig. 11. CAD model of prototype gripper designed using optimization results (best seen in color).

Based on these results, we designed the model shown in Fig. 11, which we then used to construct a prototype. The links were 3D-printed on a ProJet HD 3000 rapid prototyping machine. We used off-the-shelf torsional and linear springs, as well as ball bearings for the joints. The tendons were made from Spectra lines, commonly used for fishing or kiting; we used a model rated to 200 lbs. force. The fingers were padded with off-the-shelf rubber pads. The total cost of parts for the gripper (excluding the motor) was approximately $70.

We found the prototype gripper to exhibit all the desired characteristics. In particular, we used it to demonstrate both fingertip grasps, on objects ranging in size from the maximum finger span to a sheet of paper, and enveloping grasps, on objects with dimensions as predicted by our dimensional optimization. In addition, it can stably grasp objects of irregular shapes, or use off-center approach directions. A number of examples are shown in Fig. 12 and the video accompanying the paper. The closing sequence for both a fingertip and enveloping grasp can be seen in Fig. 1.

VI. DISCUSSION AND CONCLUSIONS

In this paper, we introduced two types of optimization and analysis for a two-finger, single-actuator gripper. Our first goal was for the gripper to achieve stable fingertip grasps, with the distal links in perfect opposition, as long as the fingers close unobstructed. In case the proximal links are stopped by contact with the object, the distal links must flex, creating stable enveloping grasps. Our second goal was to extend the range of objects that the gripper can kinematically enclose. We have shown that these goals can be achieved by a combination of optimized links dimensions and actuation parameters, including the routes of the tendons and the characteristics of the extension springs.

Fig. 12. Examples of grasps executed using prototype gripper.

We have validated this approach by constructing a prototype gripper according the results of these optimizations. The resulting end-effector can perform fingertip and enveloping grasps for a wide range of objects, exhibits the desired transition between these modes, and passively adapts to the shape of the object while maintaining stable grasps.

While noting the capabilities of a gripper designed using this approach, it is important to also highlight its limitations. This end-effector is meant to explore what is possible with a relatively low-complexity design, and very affordable hardware (and, in particular, a single actuator). An understanding of the trade-offs involved can help put it to the best use in suitable applications, and inform the design of more complex versions, for cases where improved performance is necessary.

A single actuated tendon provides flexion forces for both proximal and distal joints, meaning that a combination of flexion at the proximal joint and extension at the distal joint leads to no net change in tendon length. As such, external forces acting on the grasped object that induce this combination of joint motions are not resisted by the motor, but only by friction between the object and the rubber fingerpads. Transition from fingertip to enveloping grasps happens passively, with no active sensing or grasp planning, but requires a level of friction between the object and the proximal links, reducing the range of objects that can be enclosed. The fingers are in permanent opposition, enabling fingertip grasps of very small objects but leading to collision between the distal links when trying to envelop them.

Future designs can improve performance in multiple ways. Distal links on opposite fingers that overlap with each other instead of colliding when performing enveloping grasps can enable the enclosing of smaller objects. An additional link for each finger, as in the MARS [1] or SARAH [2] hands, could improve the ability to adapt to various grasped object shapes. Independent actuation for the proximal and distal joints can increase the stability of grasps; combined with tactile sensing, it can enable enveloping grasps of a wider range of objects. We believe these features will play an important role on the way to versatile end-effectors, widely available for operation in unstructured environments.

References

[1] C. Gosselin, T. Laliberte, and T. Degoulange, "Underactuated robotic hand," in *Video Proc. of the IEEE Intl. Conf. on Robotics and Automation*, 1998.

[2] T. Laliberte, L. Birglen, and C. M. Gosselin, "Underactuation in robotic grasping hands," *Machine Intelligence & Robotic Control*, vol. 4, no. 3, pp. 1–11, 2002.

[3] L. Birglen, T. Laliberte, and C. Gosselin, *Underactuated Robotic Hands*. Springer Tracts in Advanced Robotics, 2008.

[4] S. Hirose and Y. Umetani, "The development of soft gripper for the versatile robot hand," *Mech. and Machine Theory*, vol. 13, 1978.

[5] A. Dollar and R. Howe, "Joint coupling design of underactuated grippers," in *Mechanisms and Robotics Conf.*, 2006.

[6] A. Dollar and R. Howe, "Simple, robust autonomous grasping in unstructured environments," in *IEEE Intl. Conf. on Robotics and Automation*, 2007, pp. 4693–4700.

[7] N. Ulrich, R. Paul, and R. Bajcsy, "A medium-complexity compliant end effector," in *IEEE Intl. Conf. on Robotics and Automation*, 1988.

[8] R. Kurtz and V. Hayward, "Dexterity measure for tendon actuated parallel mechanisms," in *IEEE Intl. Conf. on Advanced Robotics*, 1991.

[9] A. Bicchi and D. Prattichizzo, "Analysis and optimization of tendinous actuation for biomorphically designed robotic systems," *Robotica*, vol. 18, pp. 23–31, 2000.

[10] N. Pollard and R. Gilbert, "Tendon arrangement and muscle force requirements for humanlike force capabilities in a robotic finger," *IEEE Intl. Conf. on Robotics and Automation*, pp. 3755–3762, 2002.

[11] J. Fu and N. Pollard, "On the importance of asymmetries in grasp quality metrics for tendon driven hands," in *IEEE-RAS Intl. Conf. on Intelligent Robots and Systems*, 2006.

[12] C. Gosselin, F. Pelletier, and T. Laliberte, "An anthropomorphic underactuated robotic hand with 15 Dofs and a single actuator," *IEEE Intl. Conf. on Robotics and Automation*, 2008.

[13] C. Brown and H. Asada, "Inter-finger coordination and postural synergies in robot hands via mechanical implementation of principal components analysis," in *IEEE-RAS Intl. Conf. on Intelligent Robots and Systems*, 2007.

[14] M. C. Carrozza, G. Cappiello, S. Micera, B. B. Edin, L. Beccai, and C. Cipriani, "Design of a cybernetic hand for perception and action," *Biol. Cybern.*, vol. 95, no. 6, pp. 629–644, 2006.

[15] M. Mason and K. Salisbury, *Robot hands and the mechanics of manipulation*. MIT Press, 1985.

[16] M. Buss, H. Hashimoto, and J. Moore, "Dextrous hand grasping force optimization," *IEEE Trans. on Robotics and Automation*, vol. 12, 1996.

[17] L.-W. Tsai, *Robot Analysis*. John Wiley & Sons, 1999.

[18] L. Han, J. Trinkle, and Z. Li, "Grasp analysis as linear matrix inequality problems," *IEEE Trans. on Robotics and Automation*, vol. 16, 2000.

[19] S. Kwak, L. Blankevoort, and G. Ateshian, "A mathematical formulation for 3D quasi-static multibody models of diarthroidal joints," *Comp. Meth. in Biomech. and Biomed. Eng.*, vol. 3, pp. 41–64, 2000.

[20] M. Ciocarlie and P. Allen, "A constrained optimization framework for compliant underactuated grasping," *Mech. Sc.*, vol. 2, no. 1, 2011.